International Journal of Earth, Energy and Environmental Sciences
ISSN: 2517-942X
Vol:15, No:8, 2021

Catalytic Pyrolysis of Sewage Sludge for Upgrading Bio-Oil Quality Using Sludge-Based Activated Char as an Alternative to HZSM5

Ali Zaker, Zhi Chen

***Abstract*—**Due to the concerns about the depletion of fossil fuel sources and the deteriorating environment, the attempt to investigate the production of renewable energy will play a crucial role as a potential to alleviate the dependency on mineral fuels. One particular area of interest is generation of bio-oil through sewage sludge (SS) pyrolysis. SS can be a potential candidate in contrast to other types of biomasses due to its availability and low cost. However, the presence of high molecular weight hydrocarbons and oxygenated compounds in the SS bio-oil hinders some of its fuel applications. In this context, catalytic pyrolysis is another attainable route to upgrade bio-oil quality. Among different catalysts (i.e., zeolites) studied for SS pyrolysis, activated chars (AC) are eco-friendly alternatives. The beneficial features of AC derived from SS comprise the comparatively large surface area, porosity, enriched surface functional groups and presence of a high amount of metal species that can improve the catalytic activity. Hence, a sludge-based AC catalyst was fabricated in a single-step pyrolysis reaction with NaOH as the activation agent and was compared with HZSM5 zeolite in this study. The thermal decomposition and kinetics were invested via thermogravimetric analysis (TGA) for guidance and control of pyrolysis and catalytic pyrolysis and the design of the pyrolysis setup. The results indicated that the pyrolysis and catalytic pyrolysis contain four obvious stages and the main decomposition reaction occurred in the range of 200-600 °C. Coats-Redfern method was applied in the 2nd and 3rd devolatilization stages to estimate the reaction order and activation energy (E) from the mass loss data. The average activation energy (E_m) values for the reaction orders n = 1, 2 and 3 were in the range of 6.67-20.37 kJ/mol for SS; 1.51-6.87 kJ/mol for HZSM5; and 2.29-9.17 kJ/mol for AC, respectively. According to the results, AC and HZSM5 both were able to improve the reaction rate of SS pyrolysis by abridging the E_m value. Moreover, to generate and examine the effect of the catalysts on the quality of bio-oil, a fixed-bed pyrolysis system was designed and implemented. The composition analysis of the produced bio-oil was carried out via gas chromatography/mass spectrometry (GC/MS). The selected SS to catalyst ratios were 1:1, 2:1 and 4:1. The optimum ratio in terms of cracking the long-chain hydrocarbons and removing oxygen-containing compounds was 1:1 for both catalysts. The upgraded bio-oils with HZSM5 and AC were in the total range of C4-C17 with around 72% in the range of C4-C9. The bio-oil from pyrolysis of SS contained 49.27% oxygenated compounds while the presence of HZSM5 and AC dropped to 7.3% and 13.02%, respectively. Meanwhile, generation of value-added chemicals such as light aromatic compounds were significantly improved in the catalytic process. Furthermore, the fabricated AC catalyst was characterized by BET, SEM-EDX, FT-IR and TGA techniques. Overall, this research demonstrated that AC is an efficient catalyst in the pyrolysis of SS and can be used as a cost-competitive catalyst in contrast to HZSM5.

Z. C. is with the Department of Building, Civil, and Environmental Engineering, Concordia University, Montreal, Canada H3G 1M8 (corresponding author, e-mail: zhichen@bcee.concordia.ca).

***Keywords*—**Activated char, bio-oil, catalytic pyrolysis, HZSM5, sewage sludge.

I. Introduction

SS generation is boosted in recent years due to the hasty expansion of municipalities and industries. SS annual production in Canada is approximately 4 million tons [1]. Recently, SS has been considered as a potential renewable energy resource for the substitution of fossil fuels [2]. In general, there are two main procedures for dealing with SS waste: incineration and landfilling. However, these options are time-consuming and suffer from various drawbacks and limitations (e.g., production of greenhouse gases and restrictive environmental regulations) [4]. Hereafter, it is an urgent need for alternative technology that can simultaneously overcome these restrictions and recycle the waste into valuable products.

Pyrolysis technology can be selected as a versatile and promising route that can give the conceptual guide for the utilization of SS in an oxygen-free environment at elevated temperatures. The tremendous benefit of pyrolysis over incineration is the elimination of harmful emissions and conversion of the organic portion, mainly aliphatic, carbohydrates and protein, to value fuel or high value-added chemical products such as benzene, toluene, xylene, etc. [3]. The converted compounds can be utilized for a variety of applications as energy (bio-oil) through industrial chemicals (bio-gas) and agricultural (char) [4], [5]. No other conversion technology can generate such a wide variety of products.

The limitation of the pyrolysis is the economic feasibility of the application and the complexity of the bio-oil obtained [6], [7]. Nevertheless, the economic profitability of the pyrolysis could be sustainability upgraded if the quality of the bio-oil could be further modified. While optimization of operating parameters for the maximum yield has been carried out widely by researchers [8]-[10], the quality and utilization of bio-oil are still under development. The main differences in the bio-oil derived from pyrolysis of SS compared to petroleum fuel are the high oxygen content, high acidity, low storage stability and low heating value. This high oxygen content reduces energy density and provokes immiscibility with hydrocarbon-based fuels [11]. The presence of oxygen-containing compounds also gives rise to the inherent instability of the bio-oils and promotes

polymerization reactions that can lead to increased viscosity [2].

It is to be noted that researchers have subjected the SS to catalytic pyrolysis for generation of advanced biofuels with lower production of oxygen-containing hydrocarbons. Traditionally, zeolites have played a key role in the petrochemical industry when processing desired fuels and chemicals due to strong acidity for the carbon-carbon bond scission and of its unique pore structure [12]. Wherefore, zeolite catalyst has been investigated for upgrading pyrolysis vapors in the production of bio-based compounds through SS pyrolysis due to deoxygenation reactions of oxygenates with increasing aromatic compounds [13]. Nonetheless, the number of studies is limited and the mechanism of cracking and reforming is yet to be comprehensively understood [14], [15]. Among the zeolite-based catalysts, HZSM5 outperformed other types because of their narrow pore diameter and shape selectivity for pyrolysis vapors from SS [16]. However, zeolites are relatively expensive, and the catalyst preparation steps are time and energy-consuming; limiting their extensive application [17]. In this case, increasing attention contributed to the examination of activated carbon as a catalyst in reforming pyrolytic vapors due to their bulky surface area, porosity, and embedded active sites [18]-[20]. Zhang et al. [21] have examined the use of corn stover-derived activated carbon catalyst with phosphoric acid activation for waste plastic pyrolysis. The result showed jet fuel-ranged alkanes and aromatics production was favored by using activated carbon. Another recent study has used rice husk for the production of Fe modified AC for catalytic pyrolysis of corn cob for bio-oil production [22]. The modified catalyst indicated selectivity to value-added products such as phenol and cresol. Similarly, a char-supported metal catalyst derived from rice husk was prepared for reforming bio-oil quality [23]. Results indicated that when the vapors from biomass pyrolysis passed through metallic supported char the selectivity and the relative contents of phenol and 4-methyl-phenol increased. However, to the best of our knowledge, few studies focused on the catalytic performance of sludge-based AC. The AC derived from SS is suitable for catalytic purposes because it is easy to generate, widely available and most essentially inexpensive [24]. Notably, metal species such as Fe are dispersed in the sludge-based char matrix inherently which can eliminate the toxic and expensive synthesis procedures. The free radicals (FR) from the evolved volatiles may react with metallic elements (ME) on the surface of AC as [25]:

$$FR + AC—ME \leftrightarrow AC— FR + ME \quad (1)$$

Therefore, this study attempts to explore the feasibility of using sludge-based AC as a low-cost alternative catalyst in contrast to commercial HZSM5 in SS pyrolysis. The aim of using a catalyst is to explore the chemical composition of bio-oils obtained from pyrolysis and catalytic pyrolysis of SS in the presence of AC and HZSM5 with different ratios. In order to understand the alterations that occur during the degradation of SS, a thermal behavioral investigation using TGA was conducted. Besides, kinetic studies involved in pyrolysis and catalytic pyrolysis of SS over HZSM5 and AC were comparatively explored. Also, catalyst structural characteristics were examined to further understand the catalytic mechanism of AC.

II. Experimental Methods

A. SS Material

SS was obtained from Montreal municipal wastewater treatment plant in Quebec, Canada. It was collected from the clarifiers which are a mixture of sludge decanted at the bottom and the scum from the top of the clarifier. After in situ mechanical dewatering at the site, the dewatered sludge cakes with a surface moisture content of approximately 68% were collected for the experiment. The initial pH of SS was 6.21. SS sample was dried at 105 °C in an oven for 24 h to reduce the surface moisture content to less than 10%. According to the literature, the best particle size (p) for decomposition of volatile matter from SS mainly for high β values is in the range of $200 < p < 800$ μm [26]. The elucidation is to assure that the experiments would be conducted in the kinetic regime, eliminating mass and heat transfer effects on the results due to the low thermal conductivity of SS [27], [28]. In this case, the dried SS was pulverized and sieved into a fine powder with particle size 500 μm; then, sealed in air-tight bags and stored in the fridge.

Basic physicochemical characteristics of SS are determined by proximate and ultimate analyzes. In the proximate analysis, moisture, ash, volatile and fixed carbon were measured using ASTM (D1762-84) standard method. The ultimate analysis was conducted using a ThermoFischer Scientific Flash 2000 CHNS/O elemental analyzer. The high heating value (HHV) is the amount of energy stored in the material. To avoid expensive and inaccurate experimental procedures, an appropriate model established to date was employed to compute HHV as described [29]. According to the elemental analysis, the simplified chemical formula of the SS that derives can be written as $(CH_{1.732}N_{0.073}S_{0.0058}O_{0.52})n$. The element composition was analyzed by ICP-OES (Agilent Technologies 5100, USA). The properties of the SS are given in Table I.

B. Catalysts Preparation

In this study, two types of catalysts were explored; a commercially available zeolite catalyst ZSM5 (surface area = 425 m^2/g, Si/Al ratio = 50, p = 500 μm) and AC derived from SS. The ZSM5 was purchased from Alfa Aesar (CAS 1318-02-1) and calcined at 550 °C for 5 h in a tubular furnace to activate (HZSM5) before use.

Dried SS was homogeneously blended with NaOH pellets in a 1:1 ratio in a blender. The blend was placed in a crucible (Fisherbrand™ Porcelain Combustion Boats) and carbonized in a tubular reactor (Lindberg/Blue M Mini-Mite™ Tube Furnaces, Thermo Scientific) at 700 °C with a heating rate (β) of 10 °C/min lasting for 120 min with N_2 as carrier gas at 0.5 L/min. After the reaction was completed, the nitrogen atmosphere was maintained until the ambient temperature was reached and then the AC was collected and sealed away in the

desiccator. The produced AC was washed with 2M HCl for 4 h, and subsequently by cold and hot deionized water of 60 °C for 2 h until reaching neutral pH. The obtained AC was oven-dried at 105 °C for 24 h.

TABLE I
PROPERTIES OF SS

Proximate analysis (wt.%)	
Volatiles [a]	56.50
Ash [a]	41.00
Fixed carbon [a,b]	2.50
HHV (MJ kg $^{-1}$)	13.05
Ultimate analysis (wt.%)[a]	
C	28.89
H	4.20
N	2.48
S	0.45
O	20.39
Elemental analysis (mg/kg)[a]	
K	4600
P	14400
Ca	63800
Mg	7220
Al	26300
Fe	24800
As	7.50
Cd	5.67
Co	45.90
Cr	44.70
Cu	338
Hg	0.261
Mn	212
Mo	5.02
Ni	33.50
Pb	54.8
Se	26.3
Zn	458
Ba	208

[a] Dry basis; [b] By difference.

It is worth mentioning that among different activation methods available in the literature; chemical modification of SS with metal hydroxide agents such as NaOH and KOH has been investigated [30], [31]. Activation with metal hydroxides not only increases the surface area but also creates several oxygenated functional groups on the surface of the AC [32]. NaOH is more environmentally friendly than KOH and is deemed more economical and less corrosive for carbon activation [33]. On the other hand, there are two main chemical preparation routes to activated SS; single-step and two-step procedures. Herein, a single-step chemical activation with NaOH was adapted since it is energetically more suitable compared to other processes [34].

C. Experimental Apparatus and Procedures

First, the pyrolysis and catalytic pyrolysis experiments were implemented in a TGA apparatus (TA-Q500). To avoid systematic errors and minimize heat and mass transfer influence, about 2.5 mg of SS was loaded into the ceramic pans for the pyrolysis experiment. In the catalytic experiments, a mixture of 2.5 mg SS and 2.5 mg catalysts was placed in the pans, in which the mass ratio of SS and mixed catalysts was nearly 1:1. The mixture of SS with HZSM5 and AC was initiated as SSHZSM5@1-1 and SSAC@1-1, respectively. Mass loss and derivative thermogravimetric (DTG) variations were recorded in the range of 30 to 1000 °C at a constant β = 10 °C/min under the argon atmosphere, to obtain a high conversion rate [35]. To ensure the reproducibility and repeatability of the data; triplicate TGA tests were performed. The maximum variation in the conversion rate (α) from sample to sample of the same materials was 0.02, and their mean value was presented in the outcomes. Then, a horizontal quartz fixed-bed reactor (700 mm length and 25 mm O.D) sealed with two flange end caps was specifically designed and implemented for this research. The furnace (Lindberg/Blue M Mini-Mite™ Tube Furnaces, Thermo Scientific) was heated electrically, and the temperature was measured using an internal thermocouple. A control program was used to manage dwell time, final temperatures and heating rate. A schematic diagram of the fixed-bed pyrolysis system is shown in Fig. 1.

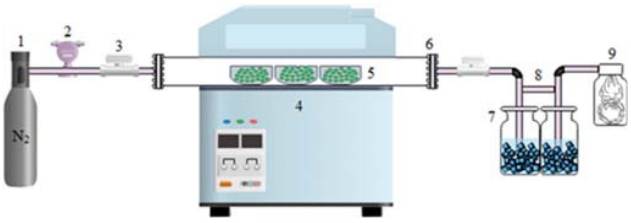

Fig. 1 Schematic of horizontal fixed bed pyrolysis reactor system. (1) Nitrogen cylinder, (2) Flowmeter, (3) Valve, (4) Furnace, (5) Crucible containing sample,(6) Quartz tube with flanges on both sides, (7) Ice bath, (8) Vacuum trap, (9) Gasbag

Three different SS to catalyst ratios with a fixed SS loading of 5 g were tested. The ratios of SS to catalysts were 4:1 initiated as SSHZSM5@4-1 and SSAC@4-1; 2:1 initiated as SSHZSM5@2-1 and SSAC@2-1; and the aforementioned SSHZSM5@1-1 and SSAC@1-1. In each experiment, approximately 10 g of the samples were added into a ceramic boat (Fisherbrand™ Porcelain Combustion Boats) which was then placed inside the furnace with a continuous flow of high-purity nitrogen through the reactor (0.5 L/min) before each experiment for 20 min. After that, the temperature of the furnace was elevated to a pre-set temperature with a heating rate of 30 °C/min with a nitrogen flow throughout the experiments to direct the pyrolysis vapors towards the condensers. The exit tube from the reactor was connected to a condensation sequence through a short connection tube (~5 cm) to avoid condensation of the hot pyrolytic volatiles before reaching the condensers. The condensation sequence consists of two vacuum traps (Synthware™ Vacuum Trap with Hose Connection on Side and Top) immersed in a water-ice bath and contained dichloromethane (DCM) to collect the liquid product. The non-condensable portion of pyrolysis gas was collected as the bio-gas in Tedler sample gasbag.

The operating parameters selected for the pyrolysis of SS were optimized through literature review and based on the TGA

results with the objective of generation of higher yield of liquid. It was observed that a dwell time of 60 min, a heating rate of 30 °C/min and a final temperature of 550 °C is an optimal condition. Also, a flow meter (Riteflow® Panel/Bench Mounted Flowmeters) was used to control the gas flow of nitrogen. The residence time (RT, s) of pyrolytic vapors inside the horizontal reactor was assessed from [36]:

$$\text{Residence Time (RT)}=V/Q \quad (2)$$

where, V is the volume of the reactor in the heating zone (V, 0.000147262 m^3) and the Q is the volumetric flow rate of the nitrogen gas (Q, 0.00000833 m^3/s). The computed residence time was approximately 17 s.

D. Sampling and Analyses

The pyrolytic liquid was filtered and diluted 5 times with DCM before composition analysis with Agilent 7890 GC/MS with an HP-5 MS capillary column. Helium was used as the carrier gas at a flow rate of 1.2 mL/min. The injection size was 1 lL with a split ratio of 1:10. The oven temperature was 40 °C initially held for 3 min and then increased to 290 °C at a rate of 5 °C/min and held at 290 °C for 5 min. The temperatures of the injector and detector were maintained at 250 and 230 °C, respectively. The compounds were identified by comparing their mass spectra with those from the National Institute of Standards and Technology (NIST) mass spectral data library. Calibration was not carried out due to a large number of compounds in the pyrolytic liquid. A semi-quantitative method was used to determine the relative proportion of each compound in the liquid by calculating the chromatographic area percentage.

The thermal stability of the AC catalyst was analyzed by the TGA instrument (TA-Q500). The TGA analysis was performed using an argon atmosphere with β = 10 °C/min, from ambient temperature to 1000 °C. The morphology of AC was analyzed using an FEI Quanta 450 SEM (Thermo Fisher Scientific, USA), operating at 25 kV and equipped with an Everhart-Thornley secondary electron detector. Energy dispersive X-ray spectroscopy (EDS) was employed for the elemental composition analysis using FEI Quanta 450 SEM equipped with an INCA microanalytical system (Oxford Instruments, UK). The surface area was measured from N_2 isotherms at -196.15 °C using a gas sorption analyzer (NOVA-1200; Quantachrome Corp., USA). The sample was degassed for 12 h under the inert condition at 200 °C before applying adsorption measurements. The N_2 adsorbed per gram of samples schemed versus the relative vapor pressure (P/P0) of N_2, and the data were fitted to the Brunauer-Emmett-Teller (BET) equation to compute surface area. Fourier Transform Infrared (FT-IR) spectroscopy (Thermo Scientific, 4700) was employed to evaluate the functional groups of AC. The infrared spectra were collected in a range of 4000-500 cm^{-1} with a resolution of 8 cm^{-1}. All analyses were carried out in triplicate.

III. Results and Discussion

A. Characterization of AC Catalyst

A preliminary idea about the structure of the AC was elucidated by SEM images. As displayed in Fig. 2 (a), micropore sizes were observed in the prepared sorbent. AC is composed of agglomerated carbon particles with a size ranging from tens to hundreds of nanometers in diameter. Fig. 2 (b) shows the EDX result of AC, demonstrating that there are several inorganic elements on the surface of the fabricated catalyst, such as iron, aluminum, titanium potassium, oxygen and silicon. This observation is in line with Table I data. Moreover, the BET surface area was found as 899.33 m^2/g for AC, which is greater than the values of rice husk [23] and pine sawdust [37] derived chars.

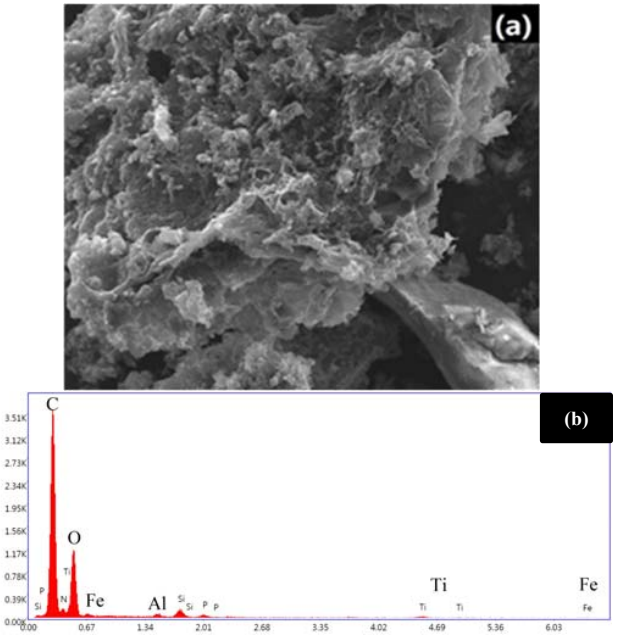

Fig. 2 (a) SEM image and (b) EDX of the AC catalyst

To identify the functional groups formed on the surface of the AC sample, FT-IR analysis was conducted as represented in Fig. 3. The functional groups detectable on the IR spectrum may be responsible for the appearance of multiple bands in a wide range of wavenumbers. In this respect, each band may have a contribution of different functional groups present on the surface of the AC. Moreover, some functional groups like -C=O and -OH are typically formed during the production of AC and have proven to have a substantial influence on catalytic activity [21], [38]. The spectra of the examined AC exhibited two bands in the 2000-4000 cm^{-1} range. The broadband centered at about 3400 cm^{-1} can be ascribed to the stretching vibration of hydrogen-bonded hydroxyl groups of water, alcohols or phenolic C-OH stretching [34]. Likewise, inorganic materials such as sulfates and phosphates are in the approximate range of 3345 and 3440 cm^{-1} [39] which is in line with the data presented in Table I. The band at about 1650 cm^{-1} is mostly the stretching vibrations of the carbonyl groups [40]. The C-H stretching is

found at 1470 cm^{-1} and the phenol O-H bending is identified at 1410 cm^{-1} [19]. The strongest peak at around 990 cm^{-1} is assigned to the C-O stretching vibration [41]. The peak at near 870 cm^{-1} can be allocated to the aromatic C-H bending vibrations [42]. The latter may be confirmed by the presence of the band at 990 cm^{-1} [39].

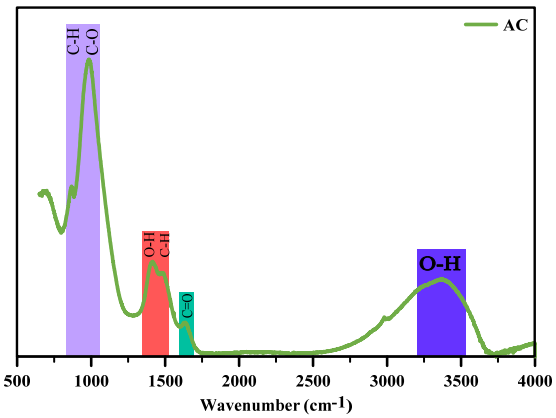

Fig. 3 FT-IR spectra of AC catalyst

To evaluate the thermal stability of the obtained AC, TGA was performed. Fig. 4 shows that the TGA/DTG curves of the AC are in good accordance with the results of a previous study [43]. Below 120 °C and due to the desorption of absorbed water, about 8% weight loss is observed. The slight weight loss of 10% recorded above 200 °C is linked to the presence of volatile compounds. The pronounced weight loss observed in the TGA analysis affirmed some functional groups such as amino and carboxyl groups existence on the surface of the AC, which is identified by FT-IR analysis [43]. Above 625 °C, the AC framework remained unchanged, indicating the high-temperature durability of AC.

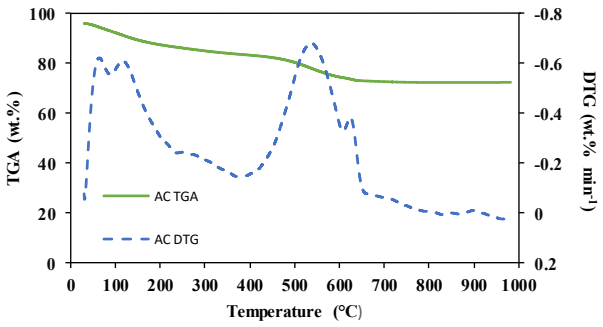

Fig. 4 TGA/DTG curves for AC catalyst

B. Thermal Decomposition Behaviors

Fig. 5 shows the TGA/DTG profiles for SS, SSHZSM5@1-1 and SSAC@1-1 samples at non-isothermal conditions. All three samples exhibit a relatively similar pattern which is consistent with the results obtained from catalytic pyrolysis of lignin over activated carbon [44] and zeolites [45]. The degradation process from the samples occurred over a wide temperature range from 30-1000 °C and was divided into 4 significant stages based on the decomposition of different components. The first stage of degradation (30-200 °C) is accompanied mostly by dehydration of organic contents by losing both free water and chemically bonded water. Stage one is not well explained in most previous literature. Usually, in the region of 120-200 °C the SS chemical structure starts to depolymerize and soften with the release of a very low quantity of light volatile compounds [46]. In this stage, the weight loss is 6.01%, 2.67% and 6.87% for SS, SSHZSM5@1-1 and SSAC@1-1, respectively. Stage 2 and 3, which are regarded as the main decomposition of reactive organic matters which are commonly named as the active stage by many researchers [15], [26]. Seemingly, the mass loss in stage 2 is 31.14%, 13.25%, and 14.53% for SS, SSHZSM5@1-1 and SSAC@1-1, respectively, due to diffuse of biodegradable organic components such as lipids and organic polymers. The DTG profiles of this stage sketched the largest peaks, which represent the maximum rate of mass loss at 352 °C, 357 °C and 358 °C for SS, SSHZSM5@1-1 and SSAC@1-1, respectively. This depicts both catalysts tend to slightly increase the temperature of the thermal degradation process. This can be explained by the behavioral similarity of the catalysts which is consistent with previous research [44], [45]. The third stage (400-600 °C) is related to the cleavage of higher molecular weight compounds into smaller ones alternative to chars formation by applying continuous heat, for instance, actively-decomposing reactions of proteins [47]. The mass loss in this stage is lower than the previous stage, with a wide flat DTG profile. The mass loss is 16.25%, 7.51% and 13.44% for SS, SSHZSM5@1-1 and SSAC@1-1, respectively. After the triplets, the degradation process came into the fourth stage, which is the decomposition of inorganic matters with a DTG peak arising from 600 to 700 °C for all samples. The sketch of the peak for SSAC@1-1 is close to SS rather than SSHZSM5@1-1 which may be ascribed to AC devolatilization, formed primarily due to the scission of terminal C-C bonds in the structure of AC [17], [48]. Also, it can contribute to the devolatilization of calcium carbonate and microcline decomposition (see Table I). Other authors presented similar trends and observations [49], [50]. After 700 °C, the mass loss rate became slow and reached a stable steady state at 1000 °C. From the obtained results, the total mass loss of SS, SSHZSM5@1-1 and SSAC@1-1 are 61.97%, 29%, and 42.58%, respectively. The lower mass loss of SSHZSM5@1-1 in contrast to SSAC@1-1 is attributed to the better thermal stability of HZSM5 in higher temperature reactions [51]. Although the presence of catalysts has abridged the mass losses, still can be beneficial by promoting selectivity on compounds of bio-oil for further research [52].

C. Reaction Kinetics Study

Valuable information can be found upon kinetic study in terms of product distribution, mass loss behavior, chemistry of the solid decomposition and thermal transfer between equipment which can be used for the optimization of pyrolysis equipment. The primary goal of pyrolysis kinetic modeling is to calculate the kinetic parameters using mathematical models, E value and pre-exponential factor (A) [53]. All kinetic

analyses go through the Arrhenius law; provide information about the rate of reaction; The rate of non-isothermal solid decomposition equation is [54]:

$$\frac{d\alpha}{dt} = k(T)f(\alpha) = A\exp\left(\frac{-E}{RT}\right)f(\alpha) \quad (3)$$

where T is the reaction temperature (K), k is the rate constant; A is the pre-exponential factor (s^{-1}), E is the activation energy (kJ/mol), and R is the universal gas constant (0.008314 kJ/molK). f(α) is the differential form of the kinetic model, where, α is a dimensionless extent of reaction term known as conversion rate and expressed as:

$$\alpha = \frac{W_0 - W_t}{W_0 - W_f} \quad (4)$$

where W_0 (mg) is the first-stage sampling weight, W_f (mg) is the weight at the end of the reaction and W_t (mg) is the weight at time t(s).

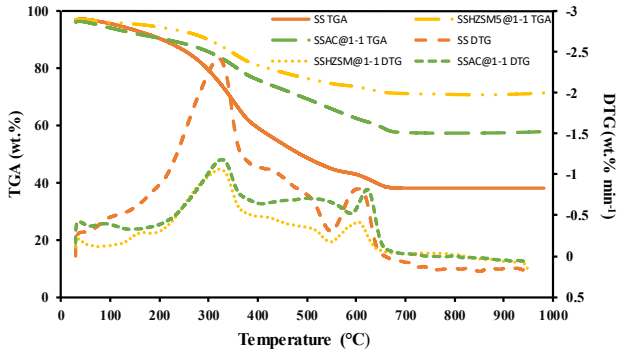

Fig. 5 TGA/DTG curves for SS, SSHZSM5@1-1 and SSAC@1-1

For a constant β=dT/dt, rearranging (2) and integrating both sides followed by taking the logarithm of the obtained equation leads to (5) and (6) which is named Coats-Redfern equation. The approximation follows as:

$$\ln\left[-\frac{\ln(1-\alpha)}{T^2}\right] = \ln\left[\frac{AR}{\beta E}\right] - \frac{E}{RT} \quad (n = 1) \quad (5)$$

and,

$$\ln\left[-\frac{1-(1-\alpha)^{1-n}}{T^2(1-n)}\right] = \ln\left[\frac{AR}{\beta E}\right] - \frac{E}{RT} \quad (n \neq 1) \quad (6)$$

This equitation can be written as a straight line (Y = mX+b), where, $\ln\left[-\frac{\ln(1-\alpha)}{T^2}\right]$ and $\ln\left[-\frac{1-(1-\alpha)^{1-n}}{T^2(1-n)}\right]$ are considered Y, respectively, and 1/T is X for easy understanding. The value of α and T at time t could be determined from the experimental TGA/DTG data. Thus, by plotting Y vs X, a straight line will be achieved. From the slope and intercept of the line, E and A values can be determined. The criteria to attain precise and satisfactory E and A values are premised on the ultimate value of n that should concede values of E with the highest coefficient of determination, R^2 to the fitted regression line. Moreover, to calculate the impacts of the HZSM5 and AC on the kinetic parameters throughout the valorization process of SS, the weighted average activation energy (E_m) was computed and applied to evaluate samples reactivity [55].

$$E = E_1F_1 + E_2F_2 + \ldots + E_nF_n \quad (7)$$

Here, E_1 to E_n are activation energy at each pyrolysis stage; and F_1 to F_n are quantities of weight losses.

Table II illustrates the E value distribution of pyrolysis and catalytic pyrolysis (with different reaction orders n = 1, 2 and 3), which were calculated by (5) and (6) for SS, SSHZSM5@1-1 and SSAC@1-1. The correlation coefficient (R^2) acknowledged the acceptable accuracy of the outcomes. The obtained results are similar to that of SS pyrolysis found by other authors by use of the same reaction mechanism [50], [56]. Since significant weight loss was found between 200-600 °C for SS, the E value was calculated for stages 2 and 3 of degradation, which is also in concurrence with other studies [57]. Likewise, E_m value was calculated to observe the catalytic activity throughout the main devolatilization stage of pyrolysis.

In the second stage of pyrolysis, 200-400 °C, it is perceived that the SS decomposition is first-order reaction (R^2 = 0.964) while for SSHZSM5@1-1 and SSAC@1-1 is third-order reaction (R2 values are 0.855 and 0.86 for SSHSZM@1-1 and SSAC@1-1, respectively). Correspondingly, presence of both catalysts has declined the E value for all three reaction orders which is in good agreement with that obtained results by other researchers [44], [51]. This low E value can be ascribed to the trivial amount of energy required to trigger the thermal degradation [52]. It is clear from Table II that the E value has dropped 10 kJ/mol for the first and second-order reaction and 15 kJ/mol for third-order reaction when AC is used as a catalyst. The decrease in the E value is more pronounced in the case of SSAC@1-1 compared to SSHZSM5@1-1 indicating higher catalytic activity at the second stage of decomposition. This phenomenon can be explained by the fact that SSAC@1-1 possesses a higher surface area. Thus, it is more favorable to the distribution of active sites of AC, which accelerates the degradation process of SS pyrolytic volatiles [21], [23]. Furthermore, the use of an activating agent causes more reactive molecules to become activated molecules. Therefore, an upsurge in the number of reactant molecules per unit volume occurs, which decreases the E value [3]. Subsequently, the best-fitted value for the order of reaction in the temperature range of 400-600 °C is calculated as n = 2 for SS (R^2 = 0.99) and n = 1 for catalytic pyrolysis (R^2 values are 0.992 and 0.952 for SSHSZM@1-1 and SSAC@1-1, respectively). In this stage of pyrolysis, the E value is lowered by the catalysts and the values for both SSHZSM5@1-1 and SSAC@1-1 are proximate. For instance, when n = 2 the E value is 26.45 and 27.75 kJ/mol for SSHZSM5@1-1 and SSAC@1-1, respectively, indicating a drop of around 10 kJ/mol in comparison to SS pyrolysis (33.77 kJ/mol). The reaction between AC catalyst and radicals, mainly H•, produced from the catalytic reaction is the essence of the pyrolytic vapors–AC interaction, and H• could even penetrate the AC at low temperatures [58]. This could explain the better catalytic performance of the SSAC@1-1 than SSHZSM5@1-1

at lower temperatures. The mean activation energies obtained from catalytic pyrolysis of SS with SiO_2, Al_2O_3, Fe_2O_3, and red mud are 191.1 kJ/mol, 189.8 kJ/mol, 175.6 kJ/mol, and 169.4 kJ/mol, respectively [59]. HZSM5 has been modified with Zn and Co and used for rice straw catalytic pyrolysis [52], [60]. The addition of these modified HZSM5 had an identical reaction order in which the E value is almost the same or higher than the raw material. Compared to metal oxides and modified HZSM5, catalysts used in this study proved higher catalytic activity in terms of energy saving.

TABLE II
THE RELATION BETWEEN REACTION STAGES AND E VALUES FOR SS, SSHZSM5@1-1 AND SSAC@1-1

Samples	n	Stage 2 (200-400°C)		Stage 3 (400-600°C)	
		E (kJ/mol)	R^2	E (kJ/mol)	R^2
SS	1	16.59	0.96	9.28	0.98
	2	23.17	0.94	33.77	0.99
	3	30.79	0.92	66.32	0.98
SSHZSM5@1-1	1	8.08	0.83	5.84	0.99
	2	14.15	0.84	26.45	0.99
	3	21.37	0.84	53.86	0.98
SSAC@1-1	1	6.90	0.83	9.62	0.95
	2	10.97	0.85	27.75	0.94
	3	15.63	0.86	51.34	0.93

E_m values, as indicated in Fig. 6, for the three reaction orders, are estimated at 6.67 kJ/mol, 12.7 kJ/mol and 20.36 kJ/mol for SS; 1.51 kJ/mol, 3.86 kJ/mol and 6.87 kJ/mol for SSHZSM5@1-1; 2.29 kJ/mol, 5.32 kJ/mol and 9.17 kJ/mol for SSAC@1-1, respectively. The presence of catalysts increased the reaction activity, and the E_m is significantly reduced. These results confirm that sludge-based AC catalyst has almost the same performance as a commercial HZSM5 catalyst in the main devolatilization stages of SS pyrolysis. It can be attributed to the presence of metals in the sludge-based AC which can catalyze the pyrolysis vapors passing through the pores, resulting in a decrease in the E_m value [3].

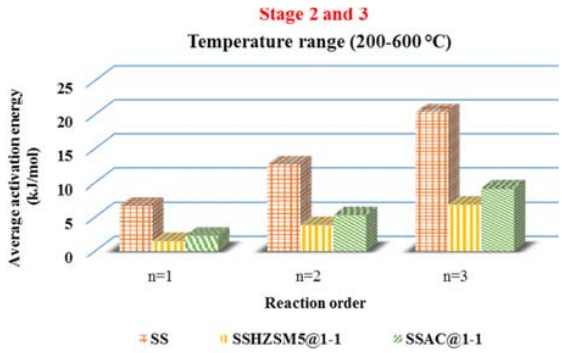

Fig. 6 The relation between reaction stages and E_m value for SS, SSHZSM5@1-1 and SSAC@1-1

D. Bio-Oil Analysis by GC/MS

Pyrolysis of SS is a very complex practice due to the mixtures in the SS bio-oil leading to a wide range of compounds in the spectrum as displayed in Fig. 7. The chemical composition of SS pyrolytic liquid obtained under the optimal condition (final temperature 550 °C, dwell time 60 min and β = 30 °C/min) from the pyrolyzer setup was analyzed for identification of organic compounds via GC/MS. Based on the spectrum data, 117 different compounds from different functional groups comprising of hydrocarbons (aliphatic or aromatic), oxygenated hydrocarbons (phenols, lipids, alcohols, acids, etc.) and nitrogenated compounds (nitriles, amines, etc.) were recorded. According to the definition of various transportation fuels, identified hydrocarbons were in the range of C4-C27 with 19.63% in the range of C4-C9; 66.21% in the range of C9-C18; and 14.49% in the range of C18-C27. Moreover, the bio-oil oxygen-containing compounds portion was more than 50% which is a detrimental property. It can affect stability and reduce the calorific value, thus, limiting the potential usage of the bio-oil for engine and turbine applications [61], [62]. Oxygenated compounds are mainly derived from extractives, lipids and polysaccharides in the SS [63]. Besides, the presence of light aliphatic aromatic compounds was around 0.71% in the derived bio-oil from SS pyrolysis and were mainly organic acids (e.g., butanoic acid, heptanoic acid, pentanoic acid, etc.). In contrast to other studies in the literature, there is no straightforward conclusion due to the heterogeneity of the SS and the operating conditions selected by the different authors. Seemingly, many authors have also pointed the presence of oxygen- and nitrogen-containing compounds and higher molecular weight hydrocarbons [64], [65]. As a result, the application of pyrolytic liquid as a fuel requires further improvements by cracking the large molecules into lower molecular weight species while reducing O and N-containing compounds. In this regard, to split heavier components into light organic oil and reduce oxygen-containing compounds, catalytic cracking process with different ratios of HZSM5 and AC has been investigated. Catalytic reforming is beneficial compared to the hydrodeoxygenation method since it does not require the addition of hydrogen and can be operated at atmospheric pressure [66]. The chemical compositions of the SSHZSM5@4-1 and SSAC@4-1 are shown in Fig. 8. The results revealed that the hydrocarbons were in the range of C4-C27 with 52.83% in the range of C4-C9; 32.8% in the range of C9-C18; and 14.38% in the range of C18-C27 for SSHZSM5@4-1. For the presence of AC catalyst, 66.26% were in the range of C4-C9; 26.11% in the range of C9-C18; and 5.61% in the range of C18-C27. The oxygenated compounds were 36.69% and 44.65% for SSHZSM5@4-1 and SSAC@4-1, respectively. Also, the proportion of value-added compounds was increased to 11% for both catalysts. The main value-added identified compounds were toluene, ethylbenzene, p-xylene and styrene. Although HZSM5 and AC had improvements in the quality of bio-oil to some extent, still the amount of oxygen-containing compounds was not acceptable for the application of bio-oil as a fuel.

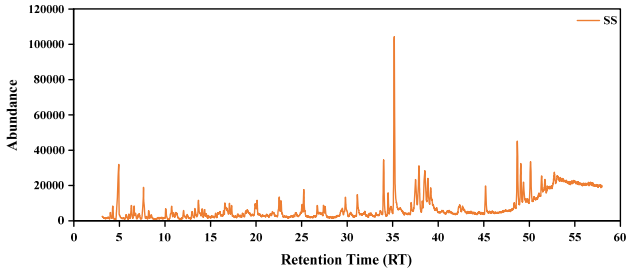

Fig. 7 Total ion chromatograms for pyrolysis of SS

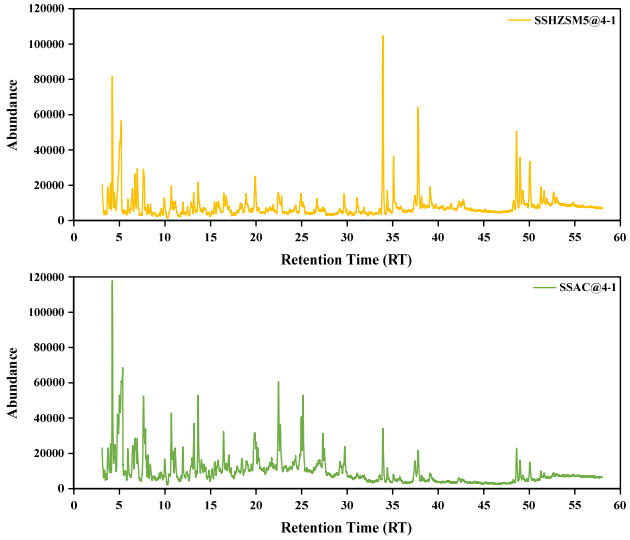

Fig. 8 Total ion chromatograms for catalytic pyrolysis of SSHZSM5@4-1 and SSAC@4-1

With the increase of catalyst to feed ratio from 4:1 to 2:1 a considerable improvement in the number of carbon atoms was not identified, as displayed in Fig. 9. However, oxygen removal was enhanced. The proportion of oxygenated compounds dropped to 20.51% and 26.76% for SSHZSM5@2-1 and SSAC@2-1, respectively. On the other hand, the production of value-added species increased to around 22% and 14% for SSHZSM5@2-1 and SSAC@2-1, respectively. The major components of bio-oils were toluene, ethylbenzene, p-xylene and 1-ethyl-2-methyl-benzene. This is in agreement with previous research on microwave-assisted pyrolysis of SS over HZSM5 presenting that the organics derived in the pyrolysis could be deoxygenated and cracked for production of aromatics [67]. The reaction mechanism and pathways can be attributed to several oxygenated compounds produced during the catalytic pyrolysis of SS which are intermediates in the production of aromatics. When the intermediates passed through the pores texture of HZSM5 and AC catalysts, some of them are altered to single-ring aromatic products through a series of oligomerization, decarboxylation, decarbonylation and dehydration reactions [68].

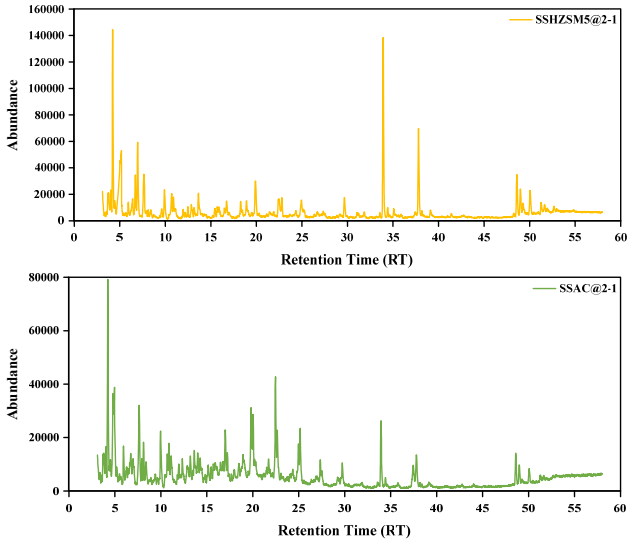

Fig. 9 Total ion chromatograms for catalytic pyrolysis of SSHZSM5@2-1 and SSAC@2-1

The analysis of bio-oil components when the SS and catalyst ratios were in the same portion is shown in Fig. 10. For both catalysts, it was noticed that the carbon numbers were in the range of C4-18 with around 73% in the range of C4-C9 and 27% in the range of C9-C18. This great range of hydrocarbon belongs to the jet fuel components [21]. Similarly, we speculated that the O-containing compounds dropped to 7.3% and 13.02% for SSHZSM5@1-1 and SSAC@1-1, respectively. In addition, the proportion of value-added chemicals in the bio-oils significantly increased to approximately 29% after catalytic cracking over HZSM5 and AC catalysts. The effect of catalysts on the formation of light hydrocarbons is related to their pore structure and acid sites [66]. The long-chain hydrocarbons (e.g., acids, alcohols, ketones, etc.) were deoxygenated and cracked into C2–C9 olefins. Then, they are converted to benzene through a series of aromatization reactions and can be transformed into other aromatics through alkylation and isomerization reactions [37], [69]. The main light hydrocarbons detected in the liquid product of SSHZSM5@1-1 were toluene, ethylbenzene, p-xylene, cyclooctatetraene and benzene, 1-ethyl-2-methyl- and for SSAC@1-1 were toluene, octene, ethylbenzene, p-xylene and styrene. The higher performance of 1:1 ratio compared to 2:1 and 4:1 is probably due to higher surface contact between pyrolysis vapors and active acid sites of catalyst particles [70]. Based on Fig. 2 (b) presence of inherent metal species in the sludge-derived AC matrix is obvious. These transition metals on the surface of AC may react with the FRs and reforming the volatiles [71]. Moreover, abundant O-containing functional groups (see Fig. 3) on the surface of AC can form some acidic centers which bind to the negatively charged π electron system of fused aromatic hydrocarbons and activate the thermal cracking reactions of those compounds in bio-oil [25]. Interestingly, proportions of nitrogenated components in the bio-oil of SSAC@1-1 were almost eliminated while for SSHZSM5@1-1 the portion was around 30%. This can be attributed to the presence of Ca and

Fe elements in the AC which can transform the nitrogenous compounds into N_2, however, more in-depth studies are required [24]. Removal of nitrogenous compounds is one of the vital targets during upgrading of SS derived bio-oils since they can lead to the release of NO_X emissions if burned as a fuel. According to the results, AC catalyst can be considered as an environmentally friendly alternative for HZSM5 substitution. Among the tested catalyst to feed ratios, 1:1 split ratio can be considered as an optimum.

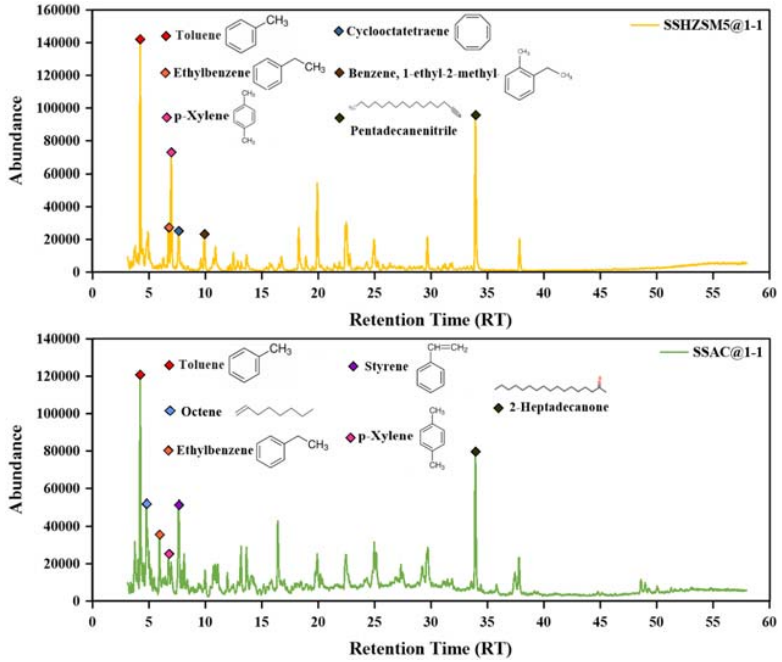

Fig. 10 Total ion chromatograms for catalytic pyrolysis of SSHZSM5@1-1 and SSAC@1-1

IV. Conclusion

In the present study, the catalytic pyrolysis of SS waste over HZSM5 and sludge-based AC as a green cost-effective alternative was invested. The catalytic pyrolysis reactions were carried out via TGA and fixed bed reactor. This study shows that both catalysts were able to reduce the E value of the process by around 10 kJ/mol. Moreover, the presence of HZSM5 proved catalytic cracking of high weight hydrocarbons to lighter species while removing oxygen-containing compounds. Besides the mentioned improvements, the fabricated AC catalyst was able to remove nitrogenous components and showed more selectivity towards production of value-added compounds. The characterization of sludge-based AC manifested porous particles which the presence of inherent metallic minerals and O-containing functional groups plays as active sites in the catalytic upgrading. The synthesis AC had a larger specific surface area and more active sites in contrast to HZSM5 resulting better catalytic performance. However, further in-depth investigation for exploring the mechanism pathways of the deoxygenation and denitrogenation of the catalytic pyrolysis reaction is recommended. Also, the effect of catalysts on the bio-char and bio-gas quality can be explored. All in all, the sludge-based AC seems to be an eco-friendly and inexpensive alternative in contrast to HZSM5 in the catalytic upgrading of SS pyrolysis bio-oil.

References

[1] A. Zaker, Z. Chen, M. Zaheer-Uddin, Catalytic pyrolysis of sewage sludge with HZSM5 and sludge-derived activated char: A comparative study using TGA-MS and artificial neural networks, Journal of Environmental Chemical Engineering. 9 (2021) 105891. doi:10.1016/j.jece.2021.105891.

[2] S.S.A. Syed-Hassan, Y. Wang, S. Hu, S. Su, J. Xiang, Thermochemical processing of sewage sludge to energy and fuel: Fundamentals, challenges and considerations, Renewable and Sustainable Energy Reviews. 80 (2017) 888–913. doi:10.1016/j.rser.2017.05.262.

[3] J. Hu, M. Danish, Z. Lou, P. Zhou, N. Zhu, H. Yuan, P. Qian, Effectiveness of wind turbine blades waste combined with the sewage sludge for enriched carbon preparation through the co-pyrolysis processes, Journal of Cleaner Production. 174 (2018) 780–787. doi:10.1016/j.jclepro.2017.10.166.

[4] M.S. Ahmad, M.A. Mehmood, S.T.H. Taqvi, A. Elkamel, C.G. Liu, J. Xu, S.A. Rahimuddin, M. Gull, Pyrolysis, kinetics analysis, thermodynamics parameters and reaction mechanism of Typha latifolia to evaluate its bioenergy potential, Bioresource Technology. 245 (2017) 491–501. doi:10.1016/j.biortech.2017.08.162.

[5] K. Wang, Y. Zheng, X. Zhu, C.E. Brewer, R.C. Brown, Ex-situ catalytic pyrolysis of wastewater sewage sludge – A micro-pyrolysis study, Bioresource Technology. 232 (2017) 229–234. doi:10.1016/j.biortech.2017.02.015.

[6] A. Zaker, Z. Chen, X. Wang, Q. Zhang, Microwave-assisted pyrolysis of sewage sludge : A review, Fuel Processing Technology. 187 (2019) 84–104. doi:10.1016/j.fuproc.2018.12.011.

[7] M.C. Samolada, A.A. Zabaniotou, Comparative assessment of municipal sewage sludge incineration, gasification and pyrolysis for a sustainable sludge-to-energy management in Greece, Waste Management. 34 (2014) 411–420. doi:10.1016/j.wasman.2013.11.003.

[8] Q. Dai, X. Jiang, Y. Jiang, Y. Jin, F. Wang, Y. Chi, J. Yan, A. Xu, Temperature influence and distribution in three phases of pahs in wet sewage sludge pyrolysis using conventional and microwave heating,

Energy and Fuels. 28 (2014) 3317–3325. doi:10.1021/ef5003638.
[9] X. Huang, J.P. Cao, P. Shi, X.Y. Zhao, X.B. Feng, Y.P. Zhao, X. Fan, X.Y. Wei, T. Takarada, Influences of pyrolysis conditions in the production and chemical composition of the bio-oils from fast pyrolysis of sewage sludge, Journal of Analytical and Applied Pyrolysis. 110 (2014) 353–362. doi:10.1016/j.jaap.2014.10.003.
[10] A. Jaramillo-Arango, I. Fonts, F. Chejne, J. Arauzo, Product compositions from sewage sludge pyrolysis in a fluidized bed and correlations with temperature, Journal of Analytical and Applied Pyrolysis. 121 (2016) 287–296. doi:10.1016/j.jaap.2016.08.008.
[11] I. Fonts, G. Gea, M. Azuara, J. Ábrego, J. Arauzo, Sewage sludge pyrolysis for liquid production: A review, Renewable and Sustainable Energy Reviews. 16 (2012) 2781–2805. doi:10.1016/j.rser.2012.02.070.
[12] W. Liu, C. Hu, Y. Yang, D. Tong, G. Li, L. Zhu, Influence of ZSM-5 zeolite on the pyrolytic intermediates from the co-pyrolysis of pubescens and LDPE, Energy Conversion and Management. 51 (2010) 1025–1032. doi:10.1016/j.enconman.2009.12.005.
[13] M.M. Rahman, R. Liu, J. Cai, Catalytic fast pyrolysis of biomass over zeolites for high quality bio-oil – A review, Fuel Processing Technology. 180 (2018) 32–46. doi:10.1016/j.fuproc.2018.08.002.
[14] R.N. State, A. Volceanov, P. Muley, D. Boldor, A review of catalysts used in microwave assisted pyrolysis and gasification, Bioresource Technology. 277 (2019) 179–194. doi:10.1016/j.biortech.2019.01.036.
[15] A. Zaker, Z. Chen, M. Zaheer-Uddin, J. Guo, Co-pyrolysis of sewage sludge and low-density polyethylene - A thermogravimetric study of thermo-kinetics and thermodynamic parameters, Journal of Environmental Chemical Engineering. 9 (2020). doi:10.1016/j.jece.2020.104554.
[16] H. Persson, I. Duman, S. Wang, L.J. Pettersson, W. Yang, Catalytic pyrolysis over transition metal-modified zeolites : A comparative study between catalyst activity and deactivation, Journal of Analytical and Applied Pyrolysis. 138 (2019) 54–61. doi:10.1016/j.jaap.2018.12.005.
[17] Y. Shen, P. Zhao, Q. Shao, D. Ma, F. Takahashi, K. Yoshikawa, In-situ catalytic conversion of tar using rice husk char-supported nickel-iron catalysts for biomass pyrolysis/gasification, Applied Catalysis B: Environmental. 152–153 (2014) 140–151. doi:10.1016/j.apcatb.2014.01.032.
[18] Y. Zhang, H. Lei, Z. Yang, K. Qian, E. Villota, Renewable High-Purity Mono-Phenol Production from Catalytic Microwave-Induced Pyrolysis of Cellulose over Biomass-Derived Activated Carbon Catalyst, ACS Sustainable Chemistry and Engineering. 6 (2018) 5349–5357. doi:10.1021/acssuschemeng.8b00129.
[19] P. Daorattanachai, W. Laosiripojana, A. Laobuthee, N. Laosiripojana, Type of contribution: Research article catalytic activity of sewage sludge char supported Re-Ni bimetallic catalyst toward cracking/reforming of biomass tar, Renewable Energy. 121 (2018) 644–651. doi:10.1016/j.renene.2018.01.096.
[20] X. Zhang, H. Lei, L. Zhu, M. Qian, X. Zhu, J. Wu, S. Chen, Enhancement of jet fuel range alkanes from co-feeding of lignocellulosic biomass with plastics via tandem catalytic conversions, Applied Energy. 173 (2016) 418–430. doi:10.1016/j.apenergy.2016.04.071.
[21] Y. Zhang, D. Duan, H. Lei, E. Villota, R. Ruan, Jet fuel production from waste plastics via catalytic pyrolysis with activated carbons, Applied Energy. 251 (2019) 113337. doi:10.1016/j.apenergy.2019.113337.
[22] L. Dai, Z. Zeng, X. Tian, L. Jiang, Z. Yu, Q. Wu, Y. Wang, Y. Liu, R. Ruan, Microwave-assisted catalytic pyrolysis of torrefied corn cob for phenol-rich bio-oil production over Fe modified bio-char catalyst, Journal of Analytical and Applied Pyrolysis. 143 (2019) 104691. doi:10.1016/j.jaap.2019.104691.
[23] F. Guo, X. Li, Y. Liu, K. Peng, C. Guo, Z. Rao, Catalytic cracking of biomass pyrolysis tar over char-supported catalysts, Energy Conversion and Management. 167 (2018) 81–90. doi:10.1016/j.enconman.2018.04.094.
[24] N. Gao, K. Kamran, C. Quan, P.T. Williams, Thermochemical conversion of sewage sludge: A critical review, Progress in Energy and Combustion Science. 79 (2020) 100843. doi:10.1016/j.pecs.2020.100843.
[25] D. qing Fu, X. hong Li, W. ying Li, J. Feng, Catalytic upgrading of coal pyrolysis products over bio-char, Fuel Processing Technology. 176 (2018) 240–248. doi:10.1016/j.fuproc.2018.04.001.
[26] S.R. Naqvi, R. Tariq, Z. Hameed, I. Ali, S.A. Taqvi, M. Naqvi, M.B.K. Niazi, T. Noor, W. Farooq, Pyrolysis of high-ash sewage sludge: Thermo-kinetic study using TGA and artificial neural networks, Fuel. 233 (2018) 529–538. doi:10.1016/j.fuel.2018.06.089.
[27] A. V. Bridgwater, Review of fast pyrolysis of biomass and product upgrading, Biomass and Bioenergy. 38 (2012) 68–94. doi:10.1016/j.biombioe.2011.01.048.
[28] S. Sfakiotakis, D. Vamvuka, Study of co-pyrolysis of olive kernel with waste biomass using TGA/DTG/MS, Thermochimica Acta. 670 (2018) 44–54. doi:10.1016/j.tca.2018.10.006.
[29] D.R. Nhuchhen, P. Abdul Salam, Estimation of higher heating value of biomass from proximate analysis: A new approach, Fuel. 99 (2012) 55–63. doi:10.1016/j.fuel.2012.04.015.
[30] X. Xiong, I.K.M. Yu, L. Cao, D.C.W. Tsang, S. Zhang, Y.S. Ok, A review of biochar-based catalysts for chemical synthesis, biofuel production, and pollution control, Bioresource Technology. 246 (2017) 254–270. doi:10.1016/j.biortech.2017.06.163.
[31] X. fei Tan, S. bo Liu, Y. guo Liu, Y. ling Gu, G. ming Zeng, X. jiang Hu, X. Wang, S. heng Liu, L. hua Jiang, Biochar as potential sustainable precursors for activated carbon production: Multiple applications in environmental protection and energy storage, Bioresource Technology. 227 (2017) 359–372. doi:10.1016/j.biortech.2016.12.083.
[32] T. Sizmur, T. Fresno, G. Akgül, H. Frost, E. Moreno-Jiménez, Biochar modification to enhance sorption of inorganics from water, Bioresource Technology. 246 (2017) 34–47. doi:10.1016/j.biortech.2017.07.082.
[33] A.U. Rajapaksha, S.S. Chen, D.C.W. Tsang, M. Zhang, M. Vithanage, S. Mandal, B. Gao, N.S. Bolan, Y.S. Ok, Engineered/designer biochar for contaminant removal/immobilization from soil and water: Potential and implication of biochar modification, Chemosphere. 148 (2016) 276–291. doi:10.1016/j.chemosphere.2016.01.043.
[34] A. Zubrik, M. Matik, S. Hredzák, M. Lovás, Z. Danková, M. Kováčová, J. Briančin, Preparation of chemically activated carbon from waste biomass by single-stage and two-stage pyrolysis, Journal of Cleaner Production. 143 (2017) 643–653. doi:10.1016/j.jclepro.2016.12.061.
[35] G. Liu, H. Song, J. Wu, Thermogravimetric study and kinetic analysis of dried industrial sludge pyrolysis, Waste Management. 41 (2015) 128–133. doi:10.1016/j.wasman.2015.03.042.
[36] S.D. Gunasee, B. Danon, J.F. Görgens, R. Mohee, Co-pyrolysis of LDPE and cellulose: Synergies during devolatilization and condensation, Journal of Analytical and Applied Pyrolysis. 126 (2017) 307–314. doi:10.1016/j.jaap.2017.05.016.
[37] Q. Liu, Z. Xiong, S.S.A. Syed-Hassan, Z. Deng, X. Zhao, S. Su, J. Xiang, Y. Wang, S. Hu, Effect of the pre-reforming by Fe/bio-char catalyst on a two-stage catalytic steam reforming of bio-oil, Fuel. 239 (2019) 282–289. doi:10.1016/j.fuel.2018.11.029.
[38] P. Hadi, M. Xu, C. Ning, C. Sze Ki Lin, G. McKay, A critical review on preparation, characterization and utilization of sludge-derived activated carbons for wastewater treatment, Chemical Engineering Journal. 260 (2015) 895–906. doi:10.1016/j.cej.2014.08.088.
[39] A. Zielińska, P. Oleszczuk, B. Charmas, J. Skubiszewska-Zięba, S. Pasieczna-Patkowska, Effect of sewage sludge properties on the biochar characteristic, Journal of Analytical and Applied Pyrolysis. 112 (2015) 201–213. doi:10.1016/j.jaap.2015.01.025.
[40] Q.H. Lin, H. Cheng, G.Y. Chen, Preparation and characterization of carbonaceous adsorbents from sewage sludge using a pilot-scale microwave heating equipment, Journal of Analytical and Applied Pyrolysis. 93 (2012) 113–119. doi:10.1016/j.jaap.2011.10.006.
[41] E. Antunes, J. Schumann, G. Brodie, M. V. Jacob, P.A. Schneider, Biochar produced from biosolids using a single-mode microwave: Characterisation and its potential for phosphorus removal, Journal of Environmental Management. 196 (2017) 119–126. doi:10.1016/j.jenvman.2017.02.080.
[42] R. Shahrokhi-Shahraki, C. Benally, M.G. El-Din, J. Park, High efficiency removal of heavy metals using tire-derived activated carbon vs commercial activated carbon: Insights into the adsorption mechanisms, Chemosphere. 264 (2021) 128455. doi:10.1016/j.chemosphere.2020.128455.
[43] T.A. Saleh, Naeemullah, M. Tuzen, A. Sarı, Polyethylenimine modified activated carbon as novel magnetic adsorbent for the removal of uranium from aqueous solution, Chemical Engineering Research and Design. 117 (2017) 218–227. doi:10.1016/j.cherd.2016.10.030.
[44] Q. Bu, H. Lei, M. Qian, G. Yadavalli, A thermal behavior and kinetics study of the catalytic pyrolysis of lignin, RSC Advances. 6 (2016) 100700–100707. doi:10.1039/c6ra22967k.
[45] Z. Luo, S. Wang, X. Guo, Selective pyrolysis of Organosolv lignin over zeolites with product analysis by TG-FTIR, Journal of Analytical and Applied Pyrolysis. 95 (2012) 112–117. doi:10.1016/j.jaap.2012.01.014.
[46] A.B. Hernández, F. Okonta, N. Freeman, Thermal decomposition of sewage sludge under N2, CO2 and air: Gas characterization and kinetic analysis, Journal of Environmental Management. 196 (2017) 560–568. doi:10.1016/j.jenvman.2017.03.036.

[47] Y. Lin, Y. Liao, Z. Yu, S. Fang, Y. Lin, Y. Fan, X. Peng, X. Ma, Co-pyrolysis kinetics of sewage sludge and oil shale thermal decomposition using TGA-FTIR analysis, Energy Conversion and Management. 118 (2016) 345–352. doi:10.1016/j.enconman.2016.04.004.
[48] J. Lee, K.H. Kim, E.E. Kwon, Biochar as a Catalyst, Renewable and Sustainable Energy Reviews. 77 (2017) 70–79. doi:10.1016/j.rser.2017.04.002.
[49] M.B. Folgueras, M. Alonso, R.M. Díaz, Influence of sewage sludge treatment on pyrolysis and combustion of dry sludge, Energy. 55 (2013) 426–435. doi:10.1016/j.energy.2013.03.063.
[50] S.R. Naqvi, R. Tariq, Z. Hameed, I. Ali, M. Naqvi, W.H. Chen, S. Ceylan, H. Rashid, J. Ahmad, S.A. Taqvi, M. Shahbaz, Pyrolysis of high ash sewage sludge: Kinetics and thermodynamic analysis using Coats-Redfern method, Renewable Energy. 131 (2019) 854–860. doi:10.1016/j.renene.2018.07.094.
[51] Z. Xiang, J. Liang, H.M. Morgan, Y. Liu, H. Mao, Q. Bu, Thermal behavior and kinetic study for co-pyrolysis of lignocellulosic biomass with polyethylene over Cobalt modified ZSM-5 catalyst by thermogravimetric analysis, Bioresource Technology. 247 (2018) 804–811. doi:https://doi.org/10.1016/j.biortech.2017.09.178.
[52] J. Liang, H.M. Morgan, Y. Liu, A. Shi, H. Lei, H. Mao, Q. Bu, Enhancement of bio-oil yield and selectivity and kinetic study of catalytic pyrolysis of rice straw over transition metal modified ZSM-5 catalyst, Journal of Analytical and Applied Pyrolysis. 128 (2017) 324–334. doi:10.1016/j.jaap.2017.09.018.
[53] G. Özsin, A.E. Pütün, TGA/MS/FT-IR study for kinetic evaluation and evolved gas analysis of a biomass/PVC co-pyrolysis process, Energy Conversion and Management. 182 (2019) 143–153. doi:10.1016/j.enconman.2018.12.060.
[54] G. Özsin, A.E. Pütün, Kinetics and evolved gas analysis for pyrolysis of food processing wastes using TGA/MS/FT-IR, Waste Management. 64 (2017) 315–326. doi:10.1016/j.wasman.2017.03.020.
[55] L. Huang, C. Xie, J. Liu, X. Zhang, K.L. Chang, J. Kuo, J. Sun, W. Xie, L. Zheng, S. Sun, M. Buyukada, F. Evrendilek, Influence of catalysts on co-combustion of sewage sludge and water hyacinth blends as determined by TG-MS analysis, Bioresource Technology. 247 (2018) 217–225. doi:10.1016/j.biortech.2017.09.039.
[56] Z. Hameed, Z. Aman, S.R. Naqvi, R. Tariq, I. Ali, A.A. Makki, Kinetic and Thermodynamic Analyses of Sugar Cane Bagasse and Sewage Sludge Co-pyrolysis Process, Energy and Fuels. 32 (2018) 9551–9558. doi:10.1021/acs.energyfuels.8b01972.
[57] Q. Xu, S. Tang, J. Wang, J.H. Ko, Pyrolysis kinetics of sewage sludge and its biochar characteristics, Process Safety and Environmental Protection. 115 (2018) 49–56. doi:10.1016/j.psep.2017.10.014.
[58] G. Yu, Y. Feng, D. Chen, M. Yang, T. Yu, X. Dai, In Situ Reforming of the Volatile by Char during Sewage Sludge Pyrolysis, Energy and Fuels. 30 (2016) 10396–10403. doi:10.1021/acs.energyfuels.6b01226.
[59] J. Yang, X. Xu, S. Liang, R. Guan, H. Li, Y. Chen, B. Liu, J. Song, W. Yu, K. Xiao, H. Hou, J. Hu, H. Yao, B. Xiao, Enhanced hydrogen production in catalytic pyrolysis of sewage sludge by red mud: Thermogravimetric kinetic analysis and pyrolysis characteristics, International Journal of Hydrogen Energy. 43 (2018) 7795–7807. doi:10.1016/j.ijhydene.2018.03.018.
[60] Z. Xiang, J. Liang, H.M. Morgan Jr, Y. Liu, H. Mao, Q. Bu, Thermal behavior and kinetic study for co-pyrolysis of lignocellulosic biomass with polyethylene over Cobalt modified ZSM-5 catalyst by thermogravimetric analysis, Bioresource Technology. 247 (2018) 804–811.
[61] R.O. Arazo, D.A.D. Genuino, M.D.G. de Luna, S.C. Capareda, Bio-oil production from dry sewage sludge by fast pyrolysis in an electrically-heated fluidized bed reactor, Sustainable Environment Research. 27 (2017) 7–14. doi:10.1016/j.serj.2016.11.010.
[62] H. Hassan, J.K. Lim, B.H. Hameed, Recent progress on biomass co-pyrolysis conversion into high-quality bio-oil, Bioresource Technology. 221 (2016) 645–655. doi:10.1016/j.biortech.2016.09.026.
[63] J. Alvarez, G. Lopez, M. Amutio, M. Artetxe, I. Barbarias, A. Arregi, J. Bilbao, M. Olazar, Characterization of the bio-oil obtained by fast pyrolysis of sewage sludge in a conical spouted bed reactor, Fuel Processing Technology. 149 (2016) 169–175. doi:10.1016/j.fuproc.2016.04.015.
[64] M. Tomasi Morgano, H. Leibold, F. Richter, D. Stapf, H. Seifert, Screw pyrolysis technology for sewage sludge treatment, Waste Management. 73 (2018) 487–495. doi:10.1016/j.wasman.2017.05.049.
[65] T.N. Trinh, P.A. Jensen, D.J. Kim, N.O. Knudsen, H.R. Sørensen, Influence of the pyrolysis temperature on sewage sludge product distribution, bio-oil, and char properties, Energy and Fuels. 27 (2013) 1419–1427. doi:10.1021/ef301944r.
[66] T.L. Liu, J.P. Cao, X.Y. Zhao, J.X. Wang, X.Y. Ren, X. Fan, Y.P. Zhao, X.Y. Wei, In situ upgrading of Shengli lignite pyrolysis vapors over metal-loaded HZSM-5 catalyst, Fuel Processing Technology. 160 (2017) 19–26. doi:10.1016/j.fuproc.2017.02.012.
[67] Q.L. Xie, P. Peng, S.Y. Liu, M. Min, Y.L. Cheng, Y.Q. Wan, Y. Li, X.Y. Lin, Y.H. Liu, P. Chen, R. Ruan, Fast microwave-assisted catalytic pyrolysis of sewage sludge for bio-oil production, Bioresource Technology. 172 (2014) 162–168. doi:10.1016/j.biortech.2014.09.006.
[68] S. Liu, Y. Zhang, L. Fan, N. Zhou, G. Tian, X. Zhu, Y. Cheng, Y. Wang, Y. Liu, P. Chen, R. Ruan, Bio-oil production from sequential two-step catalytic fast microwave-assisted biomass pyrolysis, Fuel. 196 (2017) 261–268. doi:10.1016/j.fuel.2017.01.116.
[69] S. Ren, H. Lei, L. Wang, Q. Bu, S. Chen, J. Wu, Hydrocarbon and hydrogen-rich syngas production by biomass catalytic pyrolysis and bio-oil upgrading over biochar catalysts, RSC Advances. 4 (2014) 10731–10737. doi:10.1039/c4ra00122b.
[70] Q. Xie, M. Addy, S. Liu, B. Zhang, Y. Cheng, Y. Wan, Y. Li, Y. Liu, X. Lin, P. Chen, R. Ruan, Fast microwave-assisted catalytic co-pyrolysis of microalgae and scum for bio-oil production, Fuel. 160 (2015) 577–582. doi:10.1016/j.fuel.2015.08.020.
[71] H. Wu, D.M. Quyn, C.-Z. Li, Volatilisation and catalytic effects of alkali and alkaline earth metallic species during the pyrolysis and gasification of Victorian brown coal. Part III. The importance of the interactions between volatiles and char at high temperature, Fuel. 81 (2002) 1033–1039. doi:https://doi.org/10.1016/S0016-2361(02)00011-X.